Bull. Disas. Prev. Res. Inst. Kyoto Univ., Vol. 28, Part 1, No. 254, April 1978

Mechanical Model of Particulate Material Based on Markov Process

By Sakuro MURAYAMA and Ryosuke KITAMURA

(Manuscript received April 28, 1978)

Abstract

In this paper a mechanical model for particulate materials, such as sand, is proposed to analyse their stress-strain behaviours during shear. In modelling, the motion of individual particles is assumed to be a Markov process, which is one of the well-known stochastic processes, because the irregularity of particles in both shape and volume, and the complicated fabric of particulate material are considered to prohibit the deterministic approach to the motion of individual particles in a particulate material. The strain of the particulate material is then derived by the motion of particles. It is shown that the stress-strain relationships of a particulate material derived from the proposed model compare favorably with those of Toyoura sand which are obtained from the drained compression tests and the proposed model can comprehensively evaluate the inherent anisotropy due to the fabric of particulate material, the extrinsic anisotropy due to the stress history and the non-linearity of stress-strain relationship.

1. Introduction

The problems of settlement, landslide, liquefaction and failure of embankment, and the development of the finite element method by the computer realize recently that one of the most essential subjects in soil mechanics is to establish the general stress-strain relationship of soil. For the last two decades theoretical and experimental studies have been carried out in order to obtain the stress-strain relationship. Basically, these studies are divided into two approaches, one of which is the macroscopic approach in which soil is regarded as an elastic or a plastic or an elasto-plastic or a visco-elasto-plastic body and the other is the microscopic approach in which soil is regarded as an assembly of rigid particles. In this paper the authors adopt the latter approach and attempt to clarify the deformation characteristics of particulate material such as sand by regarding the motion of individual particles as a Markov process. In what follows the coefficients in the basic equation of the Markov process are determined by using the concepts of the potential wall and the potential slip plane, and the stress-strain relationship of a particulate material will be derived by solving the basic equation of the Markov process.

2. Application of the Markov process to mechanical behaviour of particulate materials

2.1. Basic equation of the Markov process

The basic equation of the n-dimensional Markov process is expressed as follows:

$$\frac{\partial}{\partial s} w(\eta, s) = -\sum_{i=1}^{n} \frac{\partial}{\partial y_i}[A_i(\eta, s) w(\eta, s)] + \sum_{i,j=1}^{n} \frac{\partial^2}{\partial y_i \partial y_j}[B_{ij}(\eta, s) w(\eta, s)] \tag{1}$$

where η; a point $(y_1, y_2, \cdots, y_n)$ of the n-dimensional space,
s; time,
$w(\eta, s)$; the probability density function of η at the time s,
A_i and B_{ij}; the coefficients depending on η and s.

In the application of the Markov process all factors that make possible contributions to the deformation of a particulate material must be considered as random variables. However, this procedure is considered to lead to mathematical difficulties in solving Eq. (1). Therefore, as a random variable, we will adopt the factor which is considered to contribute most significantly to the deformation of a particulate material. In this respect, the direction of the normals to the tangential contact planes between particles in the particulate material are chosen here as the random variable. As a consequence of this, the motion of particles which causes the deformation of particulate material is replaced by the change in the direction of the normals.

Figure 1 shows the tangential contact plane of the two adjacent particles and the reference frame adopted. The angles between the normal line of the tangential contact plane and the reference axes, x_1, x_2 and x_3 are denoted by β_1, β_2 and β_3, respectively. Since the tangential contact plane is specified by two of the three direction cosines, we adopt contact angles β_1 and β_2, as the independent random variables. Furthermore, it is possible to replace the time s in Eq. (1) by the stress ratio in the shearing process. Thus Eq. (1) can be rewritten in the following form.

$$\frac{\partial}{\partial s} w(\eta. s) = -\sum_{i=1}^{2} \frac{\partial}{\partial \beta_i}[A_i(\eta, s) w(\eta, s)] + \sum_{i=1}^{2} \frac{\partial^2}{\partial \beta_i^2}[B_{ii}(\eta, s) w(\eta, s)] \tag{2}$$

$$A_i(\eta, s) = \lim_{\Delta \to 0} \frac{1}{\Delta} \int_0^{2\pi} \int_0^{\pi/2} (\beta_{i,s+\Delta} - \beta_{i,s}) P(\eta_s, \eta_{s+\Delta}) d\beta_{1,s+\Delta} \cdot d\beta_{2,s+\Delta} \tag{3}$$

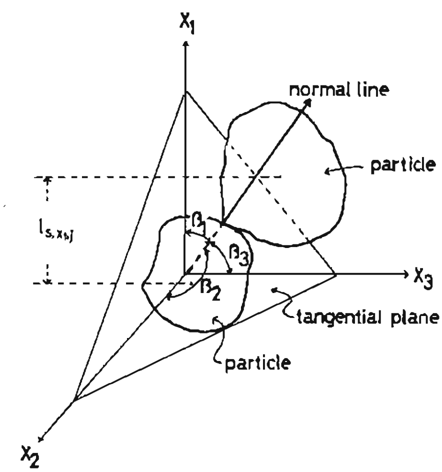

Fig. 1. Relation between two adjacent particles.

$$B_{ii}(\eta, s)=\lim_{\Delta\to 0}\frac{1}{2\Delta}\int_0^{2\pi}\int_0^{\pi/2}(\beta_{i,s+\Delta}-\beta_{i,s})^2 P(\eta_s, \eta_{s+\Delta})d\beta_{1,s+\Delta}\cdot d\beta_{2,s+\Delta} \tag{4}$$

where $w(\eta, s)$; the probablity density function of contact angle $\eta=(\beta_1, \beta_2)$ at the stress ratio s.

$P(\eta_s, \eta_{s+\Delta})$; the transition probability that contact angle changes from η_s to $\eta_{s+\Delta}$ when the stress ratio changes from s to $s+\Delta$.

2.2 Method to determine coefficients A_i and B_{ii}

It is necessary to determine the coefficients A_i and B_{ii} in order to solve Eq. (2). It should also be noted that the coefficients A_i and B_{ii}, defined by Eqs. (3) and (4), correspond to the mean value and the variance with respect to the change of contact angles which occur when the stress ratio changes. Therefore, the coefficients A_i and B_{ii} are found to represent the mechanical properties of particulate material at conatct points of adjacent particles in the shearing process as the Markov process. In order to determine these statistical quantities, A_i and B_{ii}, from the physical view point, we will introduce the concepts of the potential wall and the potential slip plane.

First, we will briefly explain the nature of the potential wall. Figure 2 schematically shows the potential walls of the elastic, viscous and visco-elastic bodies on the microstructural scale. In the elastic body the potential wall is so high that the atoms composing the elastic body cannot surmount it, as shown in Fig. 2(a). Thus the elastic behaviour is exhibited by the body. However, in the viscous body the potential wall is low as shown in Fig. 2(b), the atoms composing the body can easily surmount it and the body exhibits viscous flow. Furthermore, in the visco-elastic body the height of the potential

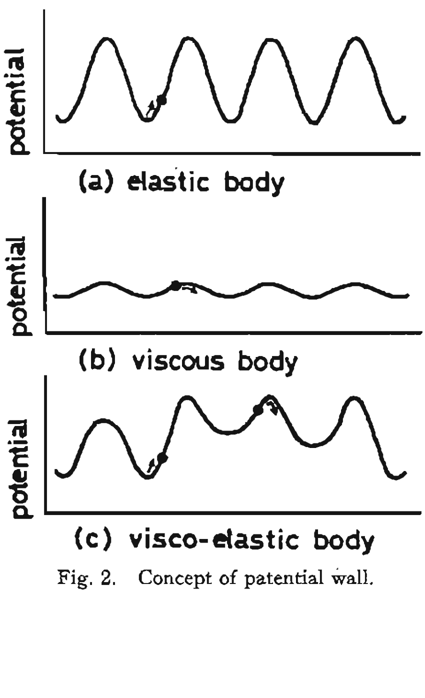

Fig. 2. Concept of patential wall.

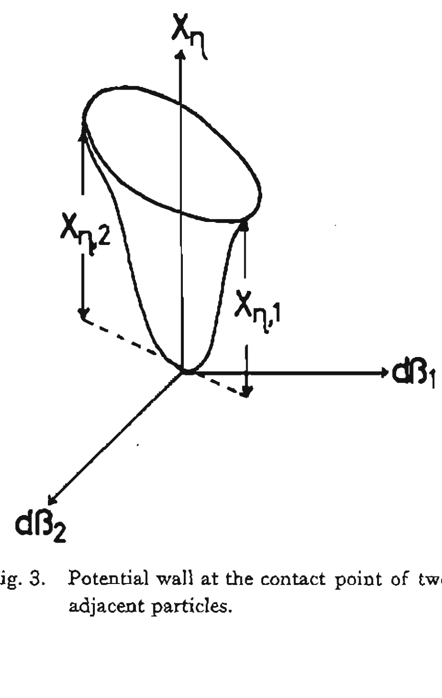

Fig. 3. Potential wall at the contact point of two adjacent particles.

wall is random as in Fig. 2(c). This is a micro-structural explanation of the visco-elastic behaviour. In the present study the micro-structural concept stated above is assumed to apply to the potential of the change in contact angle at a contact point of the two adjacent particles in a particulate material. Figure 3 schematically shows the potential wall at a contact point in the three dimensional space. The followings are assumed in the application of the potential wall to the proposed model: a recoverable change in contact angle occurs at the contact point where the activation energy cannot surmount the potential wall; and an irrecoverable change in contact angle occurs at the contact point where the activation energy can surmount the potential wall.

Let us consider combining microscopic quantities with macroscopic physical quantities by summing up the microscopic quantities. Then, the following equations are derived.

$$\sum_{\beta_1=0}^{\pi/2}\sum_{\beta_2=0}^{2\pi}(n_{\eta,1}+n_{\eta,2}+n_{\eta,0})=\sum_{\beta_1=0}^{\pi/2}\sum_{\beta_2=0}^{2\pi}n_\eta=N_c \tag{5}$$

$$\sum_{\beta_1=0}^{\pi/2}\sum_{\beta_2=0}^{2\pi}\left(n_{\eta,1}\cdot x_{\eta,1}+n_{\eta,2}\cdot x_{\eta,2}+n_{\eta,0}\cdot\frac{x_{\eta,1}+x_{\eta,2}}{2R_\eta}\right)=\Delta W \tag{6}$$

$$n_\eta=N_c\cdot w(\eta,s)d\beta_1\cdot d\beta_2 \tag{7}$$

where $x_{\eta,1}$ and $x_{\eta,2}$; the minimum and the maximum heights of a potential wall at the contact point which has the contact angle η and the irrecoverable change in contact angle as shown in Fig. 3,

$n_{\eta,1}$ and $n_{\eta,2}$; the number of contact points where the activation energy can sumrunt the potential walls, $x_{\eta,1}$ and $x_{\eta,2}$, respectively,

$n_{\eta,0}$; the number of contact points which have recoverable changes in contact angles,

N_c; the total number of contact points in the particulate material

ΔW; the work transferred into a particulate material by external forces,

R_η; the coefficient expressing the height of potential walls at the contact points which have the recoverable changes in contact angles.

Equation (6) is the energy balance equation and shows that the proposed model satisfies the first law of thermodynamics.

For later convenience, let us denote the ratios $x_{\eta,1}/x_{\eta,2}$ and $n_{\eta,2}/n_{\eta,1}$ by $R_{p,\eta}$ and $R_{n,\eta}$, respectively, i.e.,

$$x_{\eta,1}/x_{\eta,2}=R_{p,\eta} \tag{8}$$

$$n_{\eta,1}/n_{\eta,2}=R_{n,\eta} \tag{9}$$

If the probability density function of the contact angles at the contact points where the activation energy can surmount the minimum potential walls is the same in form as the probability density function of the contact angles in the whole particulate material, it then follows that

$$n_{\eta,1}=N_{c,1}\cdot w(\eta,s)d\beta_1\cdot d\beta_2 \tag{10}$$

where $N_{c,1}$; the total number of contact points where the activation energy can surmount the minimum potential wall at each contact angle.

Using Eqs. (5), (6), (8), (9) and (10), $N_{c,1}$ can be expressed as follows (see Appendix):

$$N_{c,1}=\frac{\Delta W-\sum_{\beta_1=0}^{\pi/2}\sum_{\beta_2=0}^{2\pi}\left(\frac{R_{p,\eta}+1}{2R_\eta\cdot R_{p,\eta}}\cdot x_{\eta,1}\cdot n_\eta\right)}{\sum_{\beta_1=0}^{\pi/2}\sum_{\beta_2=0}^{2\pi}\left[x_{\eta,1}\cdot w(\eta,s)d\beta_1\cdot d\beta_2\left\{\left(1+\frac{R_{n,\eta}}{R_{p,\eta}}\right)-\left(1+\frac{1}{R_{p,\eta}}\right)(1+R_{n,\eta})/2R_\eta\right\}\right]} \tag{11}$$

Substituting Eq. (11) into Eq. (10), $n_{\eta,1}$ can be expressed in terms of the quantities n_η, $x_{\eta,1}$, $w(\eta, s)$, $R_{p,\eta}$, $R_{n,\eta}$ and R_η. By using Eq. (9), $n_{\eta,2}$ can be expressed in terms of the six quantities just mentioned. Furthermore, $n_{\eta,0}$ can be obtained from Eqs. (5) and (7). The details of the method to determine n_η, $x_{\eta,1}$, $R_{p,\eta}$, $R_{n,\eta}$ and R_η will be explained and the physical meanings of these quantities will be discussed from the microscopic view point later.

Let us consider the concept of the potential slip plane.
When the stress ratio changes from the peak to the residual value in the triaxial shearing test with a particulate material, a slip plane is usually observed on the surface of the relative dense sample. The phenomenon of the formation of the slip plane is considered to be the convergence of the local slip planes, which develop randomly at the numerous contact points in a particulate material during the shearing process, to the macroscopically observable slip plane. The potential slip plane used in the proposed model means the representative plane which is composed of these numerous local slip planes and finally coincides with the macroscopically observable slip plane during the shearing process. It is also assumed here that contact planes tend to be parallel to potential slip planes. This assumption means that the probability of the occurrence of changes of contact planes proceeding in the direction of the potential slip plane is greater than the probability of the occurrence of changes of contact planes proceeding in the reverse direction of the potential slip plane.

This kind of the concept for the potential slip plane has been proposed by Murayama[1),2),3)], and Matsuoka and Nakai[4)]. Murayama applied the Mohr-Coulomb failure criterion not only to the failure but also to the shearing process preceding the failure and proposed the potential slip plane named the plane of maximum mobilization, $(\tau/\sigma)_{max}$-plane. Matsuoka and Nakai extended the $(\tau/\sigma)_{max}$-plane to the plane named the spatial mobilized plane in the three dimensional stress space. Hereafter, the spatial mobilized plane will be adopted as the potential slip plane.

With the aid of the concepts of the potential wall and the potential slip plane mentioned above, A_i and B_{ii} can be expressed as

$$A_i(\eta, s)=\frac{1}{n_\eta}(n_{\eta,1}\cdot\bar{\delta}_{\eta,1,i}+n_{\eta,2}\cdot\bar{\delta}_{\eta,2,i}+n_{\eta,0}\cdot\bar{\delta}_{\eta,0,i}), \qquad (i=1, 2) \tag{12}$$

$$B_{ii}(\eta, s)=\frac{1}{n_\eta}(n_{\eta,1}\cdot\bar{\delta}^2_{\eta,1,i}+n_{\eta,2}\cdot\bar{\delta}^2_{\eta,2,i}+n_{\eta,0}\cdot\bar{\delta}^2_{\eta,0,i}), \qquad (i=1, 2) \tag{13}$$

where $\bar{\delta}_{\eta,k,i}$ and $\bar{\delta}^2_{\eta,k,i}$; $(k=0, 1, 2)$ the mean and the mean square values of the change in contact angles at the contact points where the activation energy can surmount the potential wall,

$\bar{\delta}_{\eta,0,i}$ and $\bar{\delta}^2_{\eta,0,i}$; the mean and the mean square values of the change in contact angles at the contact points where the activation energy cannot surmount the potential wall.

Next, let us consider n_η, $x_{\eta,1}$, R_η, $R_{p,\eta}$ and $R_{n,\eta}$ in Eq. (11), and $\bar{\delta}_{\eta,k,i}$ and $\bar{\delta}^2_{\eta,k,i}$ ($i=1, 2,\ k=0, 1, 2$) in Eqs. (12) and (13).

N_c presents the total number of contact points in a particulate material and the following relations are derived.

$$N_c = \frac{C_a}{2}\cdot N_p \qquad (14) \qquad\qquad N_p = \frac{V}{1+e}\cdot\frac{1}{\bar{v}} \qquad (15)$$

where C_a; the mean value of the contact points per particle,

N_p; the total number of particles in the particulate material,

V; the volume of the particulate material,

e; the void ratio of the particulate material,

$\bar{v}$; the mean volume per particle.

Substituting Eq. (15) into Eq. (14), N_c is expressed in terms of C_a, V, e and $\bar{v}$ as

$$N_c = \frac{C_a}{2}\cdot\frac{V}{1+e}\cdot\frac{1}{\bar{v}} \qquad (16)$$

Then, n_η included in Eq. (11) is known by the use of Eq. (7).
With respect to C_a, Field[5] and Oda[6] carried out experimental studies and Field proposed the following experimental equation.

$$C_a = \frac{12}{1+e} \qquad (17)$$

In the proposed model Eq. (17) is used when C_a is calculated.

$x_{\eta,1}$, which is the minimum potential wall at the contact angle η, has the dimension [force]$\times$[length]. Therefore, the force $\boldsymbol{T}$ causing the change in contact angle and the change δ in contact angle must be obtained. First, method to determine $\boldsymbol{T}$

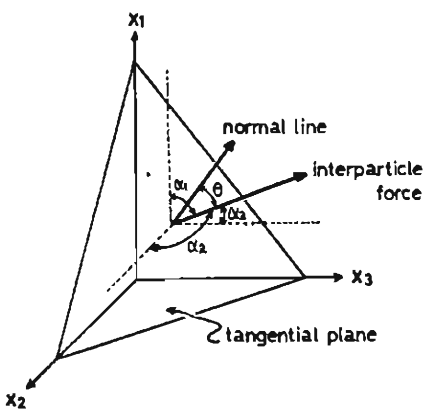

Fig. 4. Relation between the tangential plane and interparticle force at a contact point.

is described by using the interparticle force $\boldsymbol{F}$ and the frictional coefficient μ between the particles. Figure 4 shows the relation between the tangential plane and the interparticle force at a contact point. Denoting the angle between the normal line of the tangential contact plane and the direction of interparticle force by θ, $|\boldsymbol{T}|$ assums the following form:

$$\text{for } 0 \leqq \theta \leqq \tan^{-1}\mu \qquad |\boldsymbol{T}| = \mu \cdot |\boldsymbol{F}| \cdot \cos\theta \tag{18}$$

$$\text{for } \tan^{-1}\mu \leqq \theta \leqq \frac{\pi}{2} \qquad |\boldsymbol{T}| = |\boldsymbol{F}| \cdot \sin\theta \tag{19}$$

The interparticle force $\boldsymbol{F}$ is obtained by the simple average of the force and the number of contact points, i.e.,

$$|\boldsymbol{F}| = [\text{resultant force per unit area}]/[\text{the number of contact points per unit area}]$$
$$= \sqrt{\sigma_1{}^2+\sigma_2{}^2+\sigma_3{}^2} \Big/ \left\{ \frac{N_c}{(h/\bar{D})} \cdot \frac{1}{A} \right\} = A \cdot \sqrt{\sigma_1{}^2+\sigma_2{}^2+\sigma_3{}^2} \cdot \frac{h}{N_c \bar{D}} \tag{20}$$

where σ_1, σ_2 and σ_3; the principal stresses,
A; the area of cross section in the particulate material,
h; the height of the particulate material,
$\bar{D}$; the mean diameter of particles in the particulate material.

Next, let us consider the change in contact angles in the shearing process.
When the contact angle changes from $\eta = (\beta_1, \beta_2, \beta_3)$ to $\eta' = (\beta_1', \beta_2', \beta_3')$, the change, δ_η, in contact angle can be given as

$$\delta_\eta = \cos^{-1}(\cos\beta_1 \cdot \cos\beta_1' + \cos\beta_2 \cdot \cos\beta_2' + \cos\beta_3 \cdot \cos\beta_3') \tag{21}$$

Thus, the mean value of δ_η is obtained in the following form.

$$\bar{\delta}_\eta = \int_{-\infty}^{\infty} \cos^{-1}(\cos\beta_1 \cdot \cos\beta_1' + \cos\beta_2 \cdot \cos\beta_2' + \cos\beta_3 \cdot \cos\beta_3') P(\eta, \eta') d\eta' \tag{22}$$

where $P(\eta, \eta')$; the transition probability of the change in contact angle from η to η'.
Using Eqs. (18), (19), (20) and (22), $x_{\eta,1}$ is derived as follows:

$$\text{for } 0 \leqq \theta \leqq \tan^{-1}\mu \quad x_{\eta,1} = |\boldsymbol{T}| \cdot \bar{\delta}_\eta \cdot \bar{D}/2 = \mu \cdot A \cdot \sqrt{\sigma_1{}^2+\sigma_2{}^2+\sigma_3{}^2} \cdot \frac{h}{2N_c} \cdot \cos\theta \cdot \bar{\delta}_\eta \tag{23}$$

$$\text{for } \tan^{-1}\mu \leqq \theta \leqq \frac{\pi}{2} \quad x_{\eta,1} = |\boldsymbol{T}| \cdot \bar{\delta}_\eta \cdot \bar{D}/2 = A \cdot \sqrt{\sigma_1{}^2+\sigma_2{}^2+\sigma_3{}^2} \cdot \frac{h}{2N_c} \cdot \sin\theta \cdot \bar{\delta}_\eta \tag{24}$$

R_η in Eq. (6) is the coefficient which represents the height of potential walls at the contact points where the recoverable changes in contact angles occur and is related to the elastic state which means that the motion of particles in a particulate material is recoverable. Thus, in the elastic state $n_{\eta,1}$ and $n_{\eta,2}$ in Eq. (6) are equal to zero and Eq. (6) is rewritten as

$$\sum_{\beta_1=0}^{\pi/2} \sum_{\beta_2=0}^{2\pi} \{n_\eta(x_{\eta,1}+x_{\eta,2})/2R_\eta\} = \Delta W_e \tag{25}$$

where ΔW_e; the work distributed to the recoverable motion of particles.

Assuming that R_η is independent of the contact angle η, the following equation is derived from Eq. (25).

$$R_\eta = \frac{\sum_{\beta_1=0}^{\pi/2} \sum_{\beta_2=0}^{2\pi} \{n_\eta(x_{\eta,1}+x_{\eta,2})\}}{2\cdot\Delta W_e} \tag{26}$$

Let us consider $R_{p,\eta}$ defined in Eq. (8) on the basis of the relation of two adjacent particles as shown in Fig. 1.
Since the probability of change in contact angles to all directions is equal at the contact points where either β_1 or β_2 in Fig. 1 is zero or $\pi/2$, the height of the potential wall can be assumed to be constant. Thus, $R_{p,\eta}$ is unit when either β_1 or β_2 is zero or $\pi/2$. Furthermore, at all the contact points where the tangential planes are parallel to the potential slip plane (the spatial mobilized plane) the change in contact angles is considered to be the same as the change of the potential slip plane. In this case the maximum potential wall $x_{\eta,2}$ can be assumed infinite and thus $R_{p,\eta}$ is equal to zero.
The simplest function $R_{p,\eta}$ of contact angle η which satisfies the above relations between $R_{p,\eta}$ and η at the specific contact angles can be formed by the planes as shown in Fig. 5. The relation between $R_{p,\eta}$ and η shown in Fig. 5 is used in the numerical experiment.

$R_{n,\eta}$ is assumed to be the same as $R_{p,\eta}$ for simplicity in the proposed model because the ratio of the numbers of contact points, $R_{n,\eta}$, can be considered to be propotional to the ratio of the heights of the potential wall, $R_{p,\eta}$.

$\bar{\delta}_{\eta,k,i}$ in Eq. (12) and $\bar{\delta}^2_{\eta,k,i}$ in Eq. (13) which are the mean and the mean square values of the change in contact angles in the shearing process are obtained as follows: The distribution function of the change in contact angles in the shearing process is assumed to be the normal distribution function in which the mean value and the standard deviation are equal to the change of the potential slip plane. Furthermore, the concept of the potential slip plane is used to determine the direction of the change in the mean value of the distribution function.
Thus, the following equations can be given.

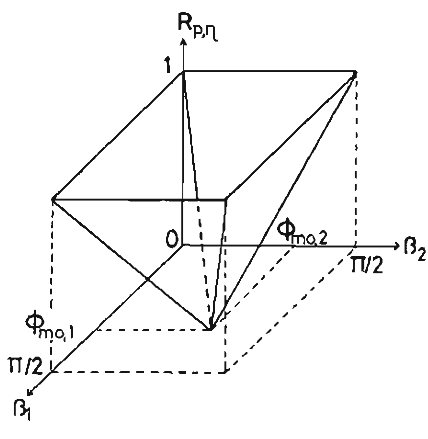

Fig. 5. Relation between $R_{p,\eta}$ and η.

for $0 \leqq \beta_i \leqq \phi_{mo,i}$ $(i=1, 2)$

$$\bar{\delta}_{\eta,0,i}=\int_{\delta_{2,i}}^{\delta_{1,i}}\delta f_{\eta,i}(\delta)d\delta \quad (27), \qquad \bar{\delta}^2_{\eta,0,i}=\int_{\delta_{2,i}}^{\delta_{1,i}}\delta^2 f_{\eta,i}(\delta)d\delta \quad (28)$$

$$\bar{\delta}_{\eta,1,i}=\int_{\delta_{1,i}}^{\infty}\delta f_{\eta,i}(\delta)d\delta \quad (29), \qquad \bar{\delta}^2_{\eta,1,i}=\int_{\delta_{1,i}}^{\infty}\delta^2 f_{\eta,i}(\delta)d\delta \quad (30)$$

$$\bar{\delta}_{\eta,2,i}=\int_{-\infty}^{\delta_{2,i}}\delta f_{\eta,i}(\delta)d\delta \quad (31), \qquad \bar{\delta}^2_{\eta,2,i}=\int_{-\infty}^{\delta_{2,i}}\delta^2 f_{\eta,i}(\delta)d\delta \quad (32)$$

where

$$f_{\eta,i}(\delta)=\frac{1}{\Delta\phi_{mo,i}\sqrt{2\pi}}\exp\left\{-\frac{(\delta-\Delta\phi_{mo,i})^2}{2(\Delta\phi_{mo,i})^2}\right\} \quad (33)$$

$\phi_{mo,i}$; the angle between the normal line of the spatial mobilitzed plane and the reference axis, x_i-axis,

$\Delta\phi_{mo,i}$; the change in $\phi_{mo,i}$ accompanied with the change of the spatial mobilized plane,

$\delta_{1,i}$ and $\delta_{2,i}$; the minimum values of the change in contact angle, β_i, at the contact points where the activation energy can surmount the minimum and the maximum potential walls respectively, and $\delta_{1,i}=\frac{3}{2}\Delta\phi_{mo,i}$ and $\delta_{2,i}=\frac{1}{2}\Delta\phi_{mo,i}$ are adopted in the numerical experiment.

for $\phi_{mo,i}<\beta_i \leqq \frac{\pi}{2}$ $(i=1, 2)$

$$\bar{\delta}_{\eta,0,i}=\int_{\delta_{1,i}}^{\delta_{2,i}}\delta f_{\eta,i}(\delta)d\delta \quad (34), \qquad \bar{\delta}^2_{\eta,0,i}=\int_{\delta_{1,i}}^{\delta_{2,i}}\delta^2 f_{\eta,i}(\delta)d\delta \quad (35)$$

$$\bar{\delta}_{\eta,1,i}=\int_{-\infty}^{\delta_{1,i}}\delta f_{\eta,i}(\delta)d\delta \quad (36), \qquad \bar{\delta}^2_{\eta,1,i}=\int_{-\infty}^{\delta_{1,i}}\delta^2 f_{\eta,i}(\delta)d\delta \quad (37)$$

$$\bar{\delta}_{\eta,2,i}=\int_{\delta_{2,i}}^{\infty}\delta f_{\eta,i}(\delta)d\delta \quad (38), \qquad \bar{\delta}^2_{\eta,2,i}=\int_{\delta_{2,i}}^{\infty}\delta^2 f_{\eta,i}(\delta)d\delta \quad (39)$$

where

$$f_{\eta,i}(\delta)=\frac{1}{\Delta\phi_{mo,i}\sqrt{2\pi}}\exp\left\{-\frac{(\delta+\Delta\phi_{mo,i})^2}{2(\Delta\phi_{mo,i})^2}\right\} \quad (40)$$

$\delta_{1,i}=-\Delta\frac{3}{2}\phi_{mo,i}$ and $\delta_{2,i}=-\frac{1}{2}\Delta\phi_{mo,i}$ are adopted in the numerical experiment.

Using the distribution function of the change in contact angles defined in Eqs. (33) and (40), $\bar{\delta}_\eta$ in Eq. (22) is given as

$$\begin{aligned}\bar{\delta}_\eta=\Delta\phi_{mo}=\cos^{-1}\{&\cos\phi_{mo,1}\cdot\cos(\phi_{mo,1}+\Delta\phi_{mo,1})\\&+\cos\phi_{mo,2}\cdot\cos(\phi_{mo,2}+\Delta\phi_{mo,2})+\cos\phi_{mo,3}\cdot\cos(\phi_{mo,3}+\Delta\phi_{mo,3})\}\end{aligned} \quad (41)$$

In the section 2.2 the physical meanings of several quantities, which are introduced in order to determine the coefficients A_i and B_{ii} in the basic equation of the Markov process are discussed. It is difficult to determine these quantities by direct measurement in the shearing test with a particulate material.

Then, the authors indirectly investigate these quantities, i.e., the quantities mentioned above are comprehensively determined so as to represent the mechanical behaviours of a particulate material which has various intial conditions and stress histories.

3. Determination of strain

When the basic equation of the Markov process, Eq. (2), is solved, the strain of a particulate material can be obtained in terms of the probability density function, $w(\eta, s)$. Figure 6 shows an element of a particulate material in the three dimensional space. The strain on the direction of x_i-axis at the stress ratio s is defined in the following form.

$$\epsilon_{s,xi}=\frac{L_{s,xi}-L_{s-\Delta s,xi}}{L_{s-\Delta s,xi}} \tag{42}$$

where $L_{s,xi}$; the length of an element in the direction of x_i-axis at the stress ratio s as shown in Fig. 6,

$L_{s-\Delta s,xi}$; the length of an element in the direction of x_i-axis at the stress ratio s-Δs.

Let us denote the number of particles in the direction of x_i-axis along the path which combines the planes facing each other at the stress ratio s as shown in Fig. 6 by $N_{s,xi}$ and the distance in the direction of x_i-axis between the centers of adjacent particles by $l_{s,xi,j}$ as shown in Fig. 1. Then the following equation is given.

$$L_{s,xi}=\sum_{j=1}^{N_{s,xi}} l_{s,xi,j} \tag{43}$$

Substitution of Eq. (43) into Eq. (42) leads to the following equation.

$$\epsilon_{s,xi}=\frac{\sum_{j=1}^{Ns,xi} l_{s,xi,j}-\sum_{j=1}^{Ns-\Delta s,xi} l_{s-\Delta s,xi,j}}{\sum_{j=1}^{Ns-\Delta s,xi} l_{s-\Delta s,xi,j}} \tag{44}$$

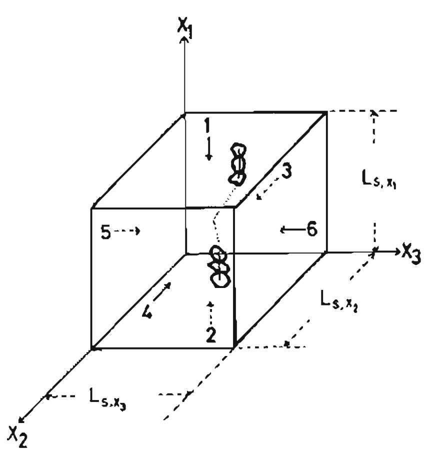

Fig. 6. Element of a particulate material.

Dividing the denominator and the numerator on the right side of this equation by $N_{s-\Delta s,xi}$, the following equation is derived.

$$\epsilon_{s,xi}=\frac{1/N_{s-\Delta s,xi}\sum_{j=1}^{Ns,xi} l_{s,xi,j}-1/N_{s-\Delta s,xi}\sum_{j=1}^{Ns-\Delta s,xi} l_{s-\Delta s,xi,j}}{1/N_{s-\Delta s,xi}\sum_{j=1}^{Ns-\Delta s,xi} l_{s-\Delta s,xi,j}}$$

$$=\frac{N_{s,xi}/N_{s-\Delta s,xi}E[l_{s,xi,j}]-E[l_{s-\Delta s,xi,j}]}{E[l_{s-\Delta s,xi,j}]} \tag{45}$$

where $E[l_{s,xi,j}]$; the mean value of $l_{s,xi,j}$ along the path in Fig. 6.

Furthermore, if the fabric of a particulate material in the direction of x_i-axis is stochastically uniform, the following equation should hold.

$$E[l_{s,xi,j}]=M[l_{s,xi,j}] \tag{46}$$

where $M[l_{s,xi,j}]$; the mean value of $l_{s,xi,j}$ in a particulate material.

$M[l_{s,xi,j}]$ can be expressed in terms of the probability density functions $w(\eta,s)$ and $g(D)$ which present the distributions of contact angles η and grain size D, i.e.,

$$M[l_{s,xi,j}]=\int_0^\infty\int_0^{2\pi}\int_0^{\pi/2} D\cdot\cos\beta_i\cdot g(D)w(\eta,s)d\beta_1\cdot d\beta_2\cdot dD$$

$$=\bar{D}\int_0^{2\pi}\int_0^{\pi/2}\cos\beta_i w(\eta,s)d\beta_1\cdot d\beta_2 \tag{47}$$

Substituting Eqs. (46) and (47) into Eq. (45), the strain $\epsilon_{s,xi}$ is given by

$$\epsilon_{s,xi}=\frac{N_{s,xi}/N_{s-\Delta s,xi}\int_0^{2\pi}\int_0^{\pi/2}\cos\beta_i w(\eta,s)d\beta_1\cdot d\beta_2-\int_0^{2\pi}\int_0^{\pi/2}\cos\beta_i w(\eta,s-\Delta s)d\beta_1\cdot d\beta_2}{\int_0^{2\pi}\int_0^{\pi/2}\cos\beta_i w(\eta,s-\Delta s)d\beta_1\cdot d\beta_2} \tag{48}$$

Eq. (48) shows that the strain which occurs due to the change in the stress ratio from $s-\Delta s$ to s can be defined in terms of $N_{s,xi}/N_{s-\Delta s,xi}$ and $w(\eta,s)$.
$N_{s,xi}/N_{s-\Delta s,xi}$, which represents the ratio of the numbers of particles along the path in the direction of x_i-axis, can evaluate the discontinuous motion of particles such as the disappearance of particles from the path and the new appearance of particles along the path. It may be reasonable, thereofre, to consider that this discontinuous motion of particles corresponds to the so-called dislocation in crystal materials.

Let us consider $N_{s,xi}/N_{s-\Delta s,xi}$ quantitatively.
It is assumed that the discontinuous motion of particles such as the disappearance of particles occurs at some of the contact points where the activation energy can surmount the potential wall. Furthermore, the discontinuous motion such as the disappearence of particles is assumed not to occur at the contact points where the tangential contact planes are horizontal (i.e., $\beta_1=0$) and to occur at all the contact points where the tangential contact planes are vertical (i.e., $\beta_1=\pi/2$).

Denoting the ratio of the discontinuous contact points to the contact points where the activation energy can surmount potential the wall by $P_d(\beta_1)$, the simplest function $P_d(\beta_1)$ which satisfies the above assumption can be given as

$$P_d(\beta_1)=\frac{(n_{\eta,1}+n_{\eta,2})_d}{(n_{\eta,1}+n_{\eta,2})}=\left(\frac{2}{\pi}\beta_1\right)^{\lambda} \tag{49}$$

where $(n_{\eta,1}+n_{\eta,2})_d$; the number of contact points where the disappearance of particles occurs,

λ; the coefficient depending on the fabric of a partculate material and stress ratio.

Then $N_{s,xi}/N_{s-\Delta s,xi}$ for the disappearance of particles can be expressed as follows

$$N_{s,xi}/N_{s-\Delta s,xi}=1-\frac{N_{s,xi}-N_{s-\Delta s,xi}}{N_{s-\Delta s,xi}}=1-\frac{\sum_{\beta_1=0}^{\pi/2}\sum_{\beta_2=0}^{2\pi}(n_{\eta,1}+n_{\eta,2})_d}{\sum_{\beta_1=0}^{\pi/2}\sum_{\beta_2=0}^{2\pi}n_\eta}$$

$$=1-\frac{1}{N_c}\sum_{\beta_1=0}^{\pi/2}\sum_{\beta_2=0}^{2\pi}\{P_d(\beta_1)\cdot(n_{\eta,1}+n_{\eta,2})\} \tag{50}$$

It is also assumed that the appearance of particles occurs at some of the contact points where the disappearance of particles occurs. Denoting this ratio by κ, $N_{s,xi}/N_{s-\Delta s,xi}$ for the appearance can be expressed as follows:

$$N_{s,xi}/N_{s\Delta-s,xi}=1+\frac{1}{N_c}\sum_{\beta_1=0}^{\pi/2}\sum_{\beta_2=0}^{2\pi}\{\kappa\cdot P_d(\beta_1)\cdot(n_{\eta,1}+n_{\eta,2})\} \tag{51}$$

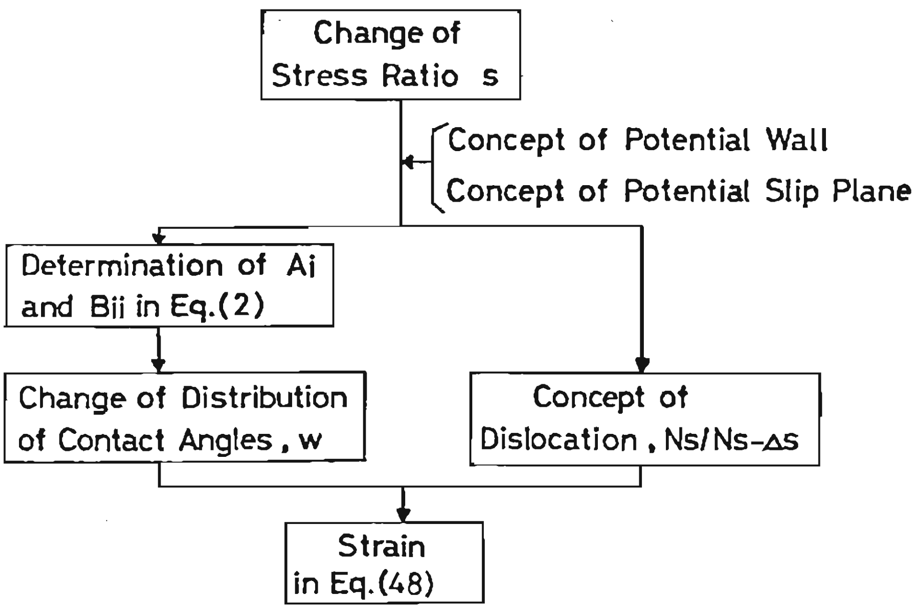

Fig. 7. Flow chart of the proposed model.

where κ; the coefficient depending on the fabric of a particulate material and stress ratio.

Figure 7 shows the essential flow chart of the proposed model which is explanied in the chapters 2 and 3. In the next chapter the numerical experiment will be carried out in accordance with this flow chart.

4. Numerical experiments

The basic equation of the Markov process, Eq. (2), was numerically solved by using the difference scheme and thus the stress-strain relationships of a particulate material were obtained. Figure 8 shows the stress-strain curves of the drained triaxial compression tests with Toyoura sand under constant radial stress and the stress-strain curves obtained

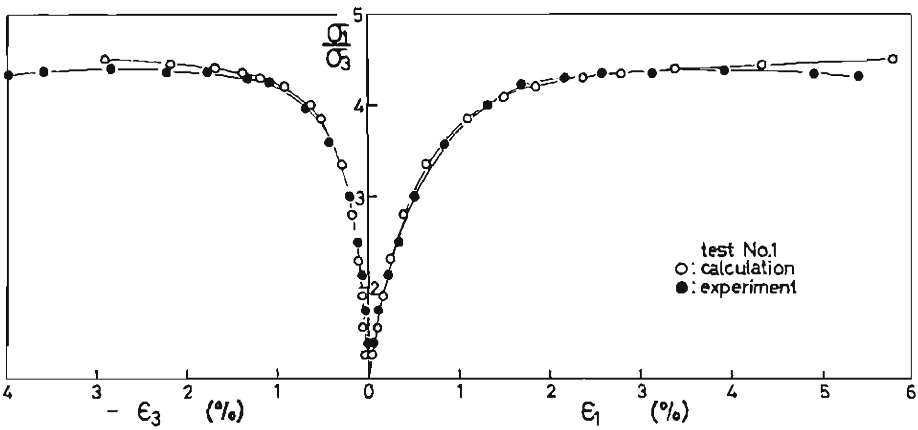

Fig. 8(a) Stress-strain curve obtained from drained triaxial compression test and numerical experiment.

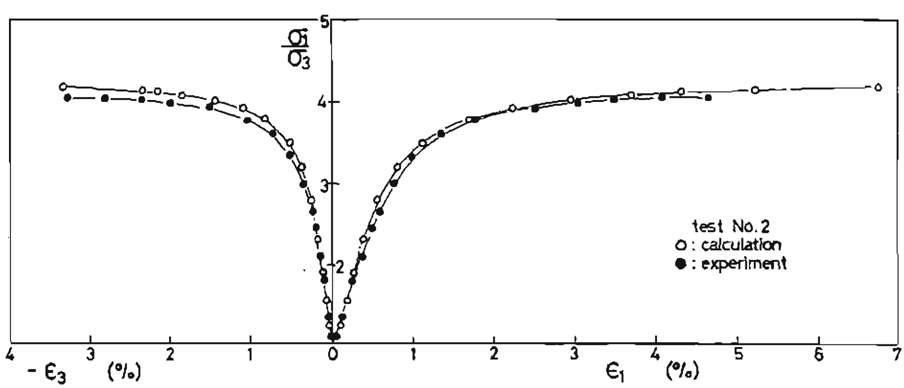

Fig. 8(b) Stress-strain curve obtained from drained triaxial compression test and numerical experiment.

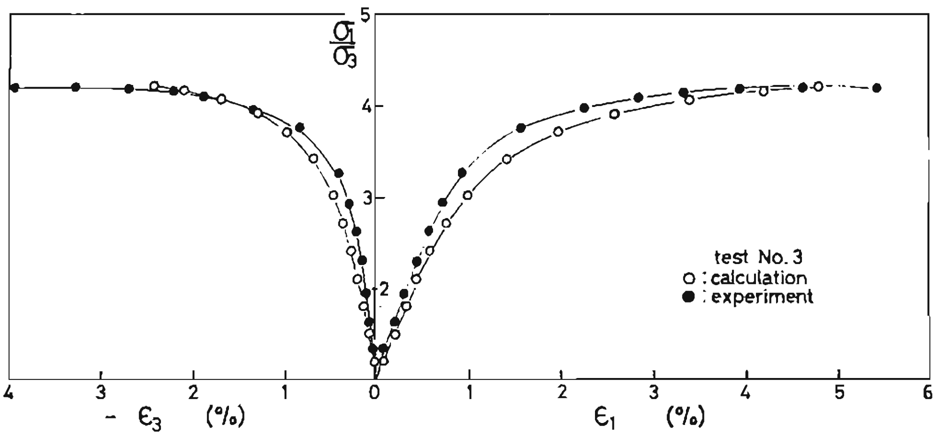

Fig. 8(c) Stress-strain curve obtained from drianed triaxial compression test and numerical experiment.

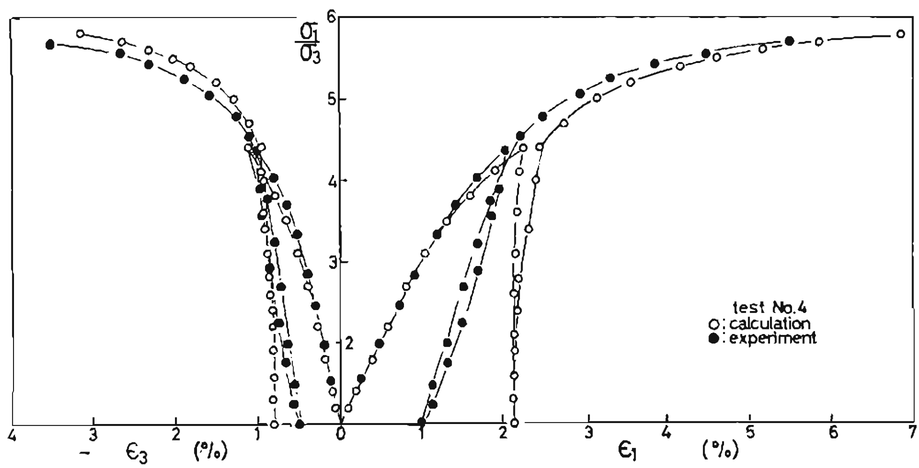

Fig. 8(d) Stress-strain curve obtained from drained triaxial compression test and numerical experiment.

Table 1. Values used in numerical experiments

Test No.	σ_3(kg/cm^2)	e_0	μ	λ	κ
1	2	0.713	0.3	$15+0.75\ (\sigma_a-\sigma_r)$	0.25
2	3	0.720	0.3	$20+1.50\ (\sigma_a-\sigma_r)$	0.20
3	4	0.716	0.3	$25+1.75\ (\sigma_a-\sigma_r)$	0.25
4	3	0.645	0.3	$15+1.50\ (\sigma_a-\sigma_r)$	0.30

σ_1: axial stress, σ_3: radial stress, e_0: initial void ratio, μ: Eq. (18), λ: Eq. (49), κ: Eq. (51)

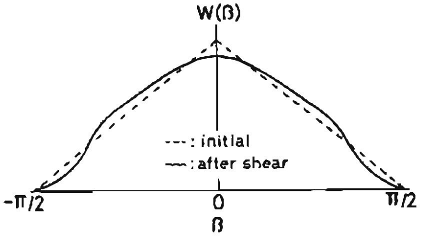

Fig. 9. Sehematic change in the distribution of contact angles during deformation process.

by numerical experiment based on the data of Toyoura sand. Table 1 shows the values used in the numerical experiments. The initial distribution of contact angles is assumed to be a triangle distribution. The change in the distribution of contact angles is schematecally shown in Fig. 9 which represents that the number of contact points which have angles near the potential slip plane increases in the shearing process because the contact angles will tend to move as to be parallel with the contact angle of the potential slip plane. It can be seen from Fig. 8 that if the initial probability density function of contact angles and the work transferred into a particulate material during the shearing process are known, the proposed model can comprehensively follow the mechanical behaviours of a real particulate material, which include the inherent anisotropy due to the complicated fabric of a particulate material, the extrinsic anisotropy due to the stress history of unloading and reloading, and the non-linearity of the stress-strain relationships.

5. Conclusion

A mechanical model for a particulate material has been developed through the microscopic approach based on the Markov process and on the concepts of the potential wall and the potential slip plane, and the stress-strain relationships associated with the model have been formulated.

The results obtained in the present paper may be summarized as follows:

(1) The application of the Markov process to the microscopic research of a particulate material is promising.

(2) The coefficients A_i and B_{ii} in the basic equation of the Markov process present the mechanical properties at the contact points in a particulate material. Thus the method of determining these coefficients exerts profound influence on the propriety of the model.

(3) the inherent anisotropy due to the fabric of a particulate material, the extrinsic anisotropy due to the stress history and the non-linearity of stress-strain relationships can be comprehensively explained by means of the proposed model.

References

1) Murayama, S.: Theoretical consideration on behaviour of sand, Proc. IUTAM Symp. on Rheology and Soil Mechanics, Grenoble, 1964, Springler-Verlag, 1966, pp.146–159.

2) Murayama, S.: Constitutive equations of particulate material in the elastic state, Preprint of Speciality Session 9, 9th Int. Conf. SMFE, 1977, pp. 167–174.

3) Murayama, S.: Constitutive equations of particulate material in the plastic state, Preprint of Speciality Session 9, 9th Int. Conf. SMFE, 1977, pp. 175–182.
4) Matsuoka, H. and Nakai, T.: Stress-deformation and strength characteristics of soil under three different principal stresses, Proc. JSCE, No. 232, Dec., 1974, pp. 59–70.
5) Field, W. G.: Towards the statistical definition of a granular mass, Proc. 4th A. and N. Z. Conf. on Soil Mech., 1963, pp. 143–148.
6) Oda, M.: Co-ordination number and its relation to shear strength of granular material, Soils and Foundations, Vol. 17, No. 2, 1977, pp. 29–42.

Appendix

Eqs. (5), (6), (8), (9) and (10) are again written below.

$$\begin{cases} n_{\eta,1}+n_{\eta,2}+n_{\eta,0}=n_\eta & (5) \\ \sum_{\beta_1=0}^{\pi/2}\sum_{\beta_2=0}^{2\pi}\left(n_{\eta,1}\cdot x_{\eta,1}+n_{\eta,2}\cdot x_{\eta,2}+n_{\eta,0}\dfrac{x_{\eta,1}+x_{\eta,2}}{2R_\eta}\right)=\Delta W & (6) \\ x_{\eta,1}/x_{\eta,2}=R_{p,\eta} & (8) \\ n_{\eta,2}/n_{\eta,1}=R_{n,\eta} & (9) \\ n_{\eta,1}=N_{c,1}\cdot w(\eta,s)d\beta_1 d\beta_2 & (10) \end{cases}$$

Eliminating $x_{\eta,2}$ and $n_{\eta,2}$ in these simultaneous equations, Eqs. (5) and (6) are rewritten as follows:

$$n_{\eta,0}=n_\eta-n_{\eta,1}(1+R_{n,\eta}) \tag{5'}$$

$$\sum_{\beta_1=0}^{\pi/2}\sum_{\beta_2=0}^{2\pi}\left\{n_{\eta,1}\cdot x_{\eta,1}+\frac{R_{n,\eta}}{R_{p,\eta}}\cdot x_{\eta,1}\cdot n_{\eta,1}+n_{\eta,0}\frac{\left(1+\dfrac{1}{R_{p,\eta}}\right)x_{\eta,1}}{2R_\eta}\right\}=\Delta W \tag{6'}$$

Furthermore, by the elimination of $n_{\eta,0}$ and $n_{\eta,1}$ in Eqs. (5'), (6') and (10), the following equation is derived.

$$\begin{aligned} N_{c,1}\cdot\sum_{\beta_1=0}^{\pi/2}\sum_{\beta_2=0}^{2\pi}&\left[x_{\eta,1}\cdot w(\eta,s)d\beta_1\cdot d\beta_2\left\{\left(1+\frac{R_{n,\eta}}{R_{p,\eta}}\right)-\left(1+\frac{1}{R_{p,\eta}}\right)(1+R_{n,\eta})/2R_\eta\right\}\right] \\ &=\Delta W-\sum_{\beta_1=0}^{\pi/2}\sum_{\beta_2=0}^{2\pi}\left\{\frac{1}{2R_\eta}\left(1+\frac{1}{R_{p,\eta}}\right)\cdot x_{\eta,1}\cdot n_\eta\right\} \end{aligned}$$

Thus, $N_{c,1}$ is given as follows:

$$N_{c,1}=\frac{\Delta W-\sum_{\beta_1=0}^{\pi/2}\sum_{\beta_2=0}^{2\pi}\left\{\dfrac{R_{p,\eta}+1}{2R_\eta\cdot R_{p,\eta}}\cdot x_{\eta,1}\cdot n_\eta\right\}}{\sum_{\beta_1=0}^{\pi/2}\sum_{\beta_2=0}^{2\pi}\left[x_{\eta,1}\cdot w(\eta,s)d\beta_1\cdot d\beta_2\left\{\left(1+\dfrac{R_{n,\eta}}{R_{p,\eta}}\right)-\left(1+\dfrac{1}{R_{p,\eta}}\right)(1+R_{n,\eta})/2R_\eta\right\}\right]}$$